
FULLERENES AND ATOMIC CLUSTERS

Atomic-Core Dynamics and the Electronic Structure of Some Endo- and Exohedral Complexes of Fullerenes with Light Elements

P. V. Avramov^{1,3}, S. A. Varganov¹, and S. G. Ovchinnikov^{1,2,3}

¹*Kirenskii Institute of Physics, Siberian Division, Russian Academy of Sciences,
Akademgorodok, Krasnoyarsk, 660036 Russia*

²*Krasnoyarsk State Technical University, Krasnoyarsk, Russia*

³*Krasnoyarsk State University, Krasnoyarsk, 660062 Russia*

e-mail: paul@post.krascience.rssi.ru

Received December 23, 1999; in final form, April 3, 2000

Abstract—The atomic and electronic structure of some endo-, exo-, and endo-exohedral complexes of the fullerene C₆₀ with various guest atoms and molecules (He_n, H₂, and Li₂) are investigated using semiempirical and nonempirical quantum-chemical methods. The atomic core dynamics is studied by the method of molecular dynamics. It is shown that guest atoms and molecules in fullerene polyhedra acquire an orbital angular momentum due to the correlated motion of nuclei above the low-energy barriers of the potential surface within the carbon polyhedron even at low temperatures (from 4 to 78 K). The emergence of orbital angular momenta of nuclei of guest atoms and molecules is attributed to a change in the contribution of the orbital angular momentum of electrons to the potential surface of the complexes. The motion of Li ions in a polyhedron leads to blurring of the top of the valence band and to the emergence of a charge polarization wave in the carbon polyhedron. © 2000 MAIK “Nauka/Interperiodica”.

A large number of compounds of fullerenes with metals are known at present (see, for example, [1–3]). These materials can be divided into two large classes: endohedral complexes, in which metal atoms are inside the fullerene polyhedra, and exohedral complexes, in which metal atoms are located outside the polyhedra. Both classes have attracted considerable attention from researchers due to their unique chemical and physical properties, including their magnetic and superconducting characteristics. The most interesting metal–fullerene objects at present are probably exo- and endohedral fullerene complexes with alkali metals. This is primarily due to the fact that compounds of the K₃C₆₀ and Rb₃C₆₀ type [1, 4] are superconductors with rather high superconducting transition temperatures approaching 55 K. An elegant method of synthesis of the endohedrals Li@C₆₀, Li₂@C₆₀, and Li₃@C₆₀, in which fullerite C₆₀ is bombarded by a beam of lithium ions with an energy up to 30 eV, was also developed recently [5].

Fullerene complexes with metals have been studied intensely for a long time by using both experimental (see, for example, [5–12]) and theoretical methods (see, for example, [1, 3, 13–27]). The electronic structure of metal complexes was studied by the method of electron spectroscopy. Weaver [9], for example, analyzed photoelectron spectra and inverse photoemission spectra of exohedral compounds of the K_xC₆₀ type (Fig. 1).

It can be seen that the filling of the lower vacant orbital of C₆₀ during doping by an alkali metal (potassium in our case) leads not only to a displacement of the occupied and vacant states, but also to a considerable change in the shape of the bands and a complex behavior of the Fermi level. A transition from pure C₆₀ to KC₆₀ leads to the disappearance of the band gap due to the formation of an impurity state on the one hand and a considerable (of the order of 1 eV) displacement of the first peak in the inverse emission spectrum on the other. A further increase in the extent of doping leads to a monotonic increase in the density of the impurity electron state, while the vacant state behaves in a more complex manner. For a doping degree of 2.5, it is displaced to the maximum extent on the energy scale (by 1.5 eV as compared to C₆₀), and then starts moving upwards along the energy scale again, and the band gap reappears for $x \approx 6$.

Another informative method of studying the electronic and atomic structures of both pure compounds and their complexes with metals is NMR and EPR spectroscopy. Almost immediately after the synthesis of the C₆₀ molecule, it was established with the help of NMR spectroscopy that C₆₀ molecules rotate in a solid at room temperature [28–30] at a frequency of the order of 10¹¹ s⁻¹ with randomly oriented rotational axes of the molecules. As the temperature is lowered to 250 K, the rotation becomes slower and ordered and the molecules now rotate only about a single axis [31, 32].

Similar results on the rotation of C_{60} molecules along a preferred axis of K_3C_{60} and Rb_3C_{60} crystals were obtained in [6] with the help of NMR spectroscopy. It was also pointed out that the freezing of rotation at a certain temperature plays an important role in the phase transitions in such materials.

Another important publication [11] in this field is also worth mentioning. Sato *et al.* [11] studied the molecular and intermolecular dynamics for solid $CeLa@C_{80}$. This compound was obtained in the course of beta decay of one of the ^{140}La atoms implanted in a carbon polyhedron. Sato *et al.* detected not only rotations of the molecules themselves, which were abruptly frozen at 160 K, but also rotations of Ce atoms, which persisted to temperatures of the order of 40 K.

The rapid migration of La ions in fullerene was also studied using the molecular dynamics method on the basis of the potential calculated in the LDA approach [33]. It was proved that La moves very rapidly along the tangent to a carbon polyhedron and performs one revolution in approximately one picosecond. Similar results were also obtained by Andreoni and Curioni [33, 34] for the endohedral $La@C_{82}$. These results led to the conclusion that the results of some experiments on the electronic and atomic structure should be interpreted taking the rotation into account. In particular, EPR spectroscopy cannot be used to extract the required information, since the characteristic time for EPR processes is an order of magnitude longer than the period of revolution of a La ion in the polyhedron.

A large number of endohedral fullerene complexes with individual atoms, as well as some molecules, have been obtained. It is obvious, however, that not all guest atoms and molecules can move in carbon polyhedra. In spite of the considerable interest of theoretical and experimental physicists in these exotic compounds, the coordination (location) of guest atoms and molecules that remain stationary in a polyhedron has not been determined in the general form. Indeed, only scant experimental information has been obtained on the structure of solids based on endohedra such as $Y@C_{82}$, for which it is known [10] that the yttrium atom is rigidly fixed to the carbon wall from inside, and endohedral molecules themselves in the molecular solid are arranged in a "head-to-tail" manner. These results were obtained, using a synchrotron source of radiation, by the methods of x-ray powder diffraction and maximum entropy. It was found that the yttrium atom is separated from the center of the C_{82} polyhedron by a distance of 3.14 Å. It was also shown that the rotation of the endohedral complex in the crystal lattice is suppressed, while C_{82} can rotate freely. The separation between the guest atom and the carbon wall in this case is approximately equal to 2.9 Å, which slightly exceeds the value predicted by quantum-chemistry methods.

For obvious reasons, the methods of coordination of guest atoms have been studied much better theoretically than experimentally. It was shown that some

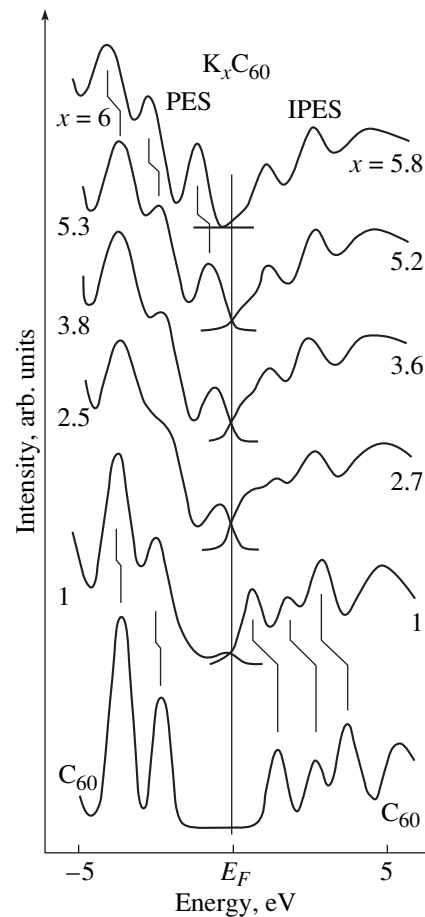


Fig. 1. Photoelectron spectra (PES) and inverse photoemission spectra (IPES) [9] of compounds of the K_xC_{60} type. For $x = 1$, the spectral intensity of the photoelectron spectrum at the Fermi level is low, while the first peak of the inverse photoemission spectrum is significant. However, the intensity of the photoelectron spectrum increases with doping, while the first peak of the inverse photoemission spectrum decreases.

atoms and ions like He and K^+ [16, 17, 25] must be coordinated at the center of a carbon polyhedron, while others, such as Li^+ and Na^+ , must be coordinated at the carbon wall [13, 16, 35]. It is clear from the most general considerations that there exist five ways of coordinating a guest atom (at the center of a hexagon, at the center of a pentagon, at the edge between two hexagons, at the edge between a pentagon and a hexagon, and at the vertex of a truncated icosahedron). Obviously, in the presence of more than one guest atom, the number of possible arrangements of atoms within a carbon tetrahedron can be even greater.

An interesting theoretical publication [4] is also worth mentioning. Ramirez [4] proved that guest atoms can tunnel between the minima of a multivalley potential surface of an inner carbon wall. However, the problem was solved in the general form by using a model Hamiltonian under the assumption that the potential

surface over which the guest atom moves has twenty minima each of which lies above the center of a hexagon. The nature of the chemical interaction between the carbon wall and the guest atom was not considered.

This work is devoted to the study of the effects associated with the “flexibility” of the atomic core of endohedral complexes and the effect of the arrangement of guest atoms in a fullerene polyhedron on the electronic structure of these compounds.

1. METHODS AND OBJECTS OF INVESTIGATION

The electronic and atomic structures and the dynamic properties of a number of fullerene complexes with Li and He atoms, as well as with a hydrogen molecule, were investigated by the standard semiempirical quantum-chemistry PM3, MNDO, and INDO methods, the nonempirical Hartree–Fock method in the 3- to 21-G basis, and the molecular dynamics method, each method employing its own calculated potential. The GAMES program [36] (electronic structure and equilibrium atomic geometry) and the demonstration version of the “HyperChem-5.02” program (electronic structure, equilibrium atomic geometry, and molecular dynamics) were used for computer calculations. Such a variety of quantum-chemical methods is necessary for the following reasons.

(1) It is necessary to verify that the potentials obtained using different quantum-chemical methods (both nonempirical and semiempirical) lead to matching results in the molecular dynamics method.

(2) Unfortunately, none of the semiempirical methods possesses a parametrization for all the atoms constituting the chosen objects.

(3) It is impossible to make molecular-dynamic calculations in the quantum-chemical *ab initio* approach even on a small basis of the 3- to 21-G type for large systems (containing several dozens of carbon atoms like the C_{60} molecule) by using the existing computer facilities. (For example, a molecular-dynamic computation of the $Li_2@C_{60}$ system by the semiempirical MNDO method disregarding the symmetry of the duration of 1 ps and a step of 0.001 ps on a P-II 450 Dual 256 MB RAM computer requires more than a week of continuous operation.)

On the other hand, the semiempirical method can be successfully used to describe the electronic structure, as well as the equilibrium atomic geometry, of the C_{60} molecule itself and its derivatives doped with alkali metals in the case when the system has a closed electron shell (see, for example, [37] and some other publications). For example, the results obtained by the Hartree–Fock method in the 3- to 21-G basis were compared in [37] with the experimental photoelectron spectra and with the results of semiempirical computations by the PM3 and MNDO methods for endo- and exohedral complexes of C_{60} with the Li^+ ion and the Li_2

dimer. It was proved that semiempirical methods give results matching with the results of nonempirical calculations and correctly describe the experimental photo-electronic data taking into account systematic errors associated with the effects of strong electron correlations in these systems. By the way, such a result is not astonishing, especially in the case of endohedral complexes. As a matter of fact, all semiempirical methods correctly describe carbon-based systems with strong chemical bonds, such as fullerenes and their endo-derivatives with alkali metals. In view of its unique electronic structure, the fullerene polyhedron is an oxidizer for alkali metals and attracts the *s* electrons of the metal. Thus, the bond in the molecule becomes mainly ionic (the charge of the alkali metal ion is of the order of +0.6). If, however, more than one guest atom (excluding the H_2 molecule) is implanted into the carbon polyhedron, the system, in addition, becomes stressed, since the internal volume is insufficient for their accommodation.

Thus, the choice of semiempirical quantum-chemical approaches for an extensive molecular-dynamic simulation of the behavior of such systems appears as justified and appropriate. In all cases, the calculated equilibrium geometry was used as the initial geometry in molecular-dynamic computations made under the assumption that the object under investigation is in a vacuum.

We analyzed the following objects.

(1) The C_{60} molecule with an icosahedral symmetry. The electronic structure and the equilibrium geometry were calculated in the restricted Hartree–Fock approximation by the nonempirical Hartree–Fock method in the 3- to 21-G basis and the semiempirical PM3 method. The length of the 6–6 bond in the *ab initio* approach and in the PM3 method amounted to 0.1367 and 0.1384 nm, respectively, while the length of the 6–5 bond was 0.1453 and 0.1457 nm, respectively. The molecular dynamics was calculated in the potential of the semiempirical PM3 method disregarding the symmetry.

(2) The C_{36} molecule with the D_{6h} symmetry. The electronic structure and the equilibrium geometry were calculated in the restricted Hartree–Fock approximation by the nonempirical Hartree–Fock method in the 3- to 21-G basis and the semiempirical PM3 method. The bond lengths in the *ab initio* approach and in the PM3 method were 0.1393 and 0.1411 nm, respectively, for the first type (6–6), 0.1438 and 0.1437 nm for the second type (6–5), 0.1415 and 0.1430 nm for the third type (6–5), and 0.1485 and 0.1499 nm for the fourth type (5–5). In order to verify these results, we made calculations in the 6- to 31-G basis and by the DFT B3LYP method. Both these calculations confirmed the correctness of computations in the 3- to 21-G basis and by the semiempirical PM3 method. The molecular dynamics was calculated using the potential

obtained by the semiempirical PM3 method and the nonempirical potential 3- to 21-G disregarding the symmetry.

(3) The endohedral complex $\text{Li}_2@C_{60}$, whose electronic structure and equilibrium geometry were calculated in the restricted Hartree–Fock approximation by the semiempirical MNDO method (a more detailed analysis of the electronic and atomic structures of this complex is given in [37]). The molecular dynamics was calculated in the potential of the semiempirical MNDO method disregarding the symmetry.

(4) The exohedral complex Li_2C_{60} , whose electronic structure and equilibrium geometry were calculated in the restricted Hartree–Fock approximation by the semiempirical MNDO method (see [37]). The molecular dynamics was calculated in the potential obtained by the semiempirical MNDO method.

(5) The endo-exohedral complex $\text{Li}[\text{Li}@C_{60}]$ (one of the ions is inside the polyhedron and the other is outside it), whose electronic structure and equilibrium geometry were calculated in the restricted Hartree–Fock approximation by the semiempirical MNDO method (see [37]). The molecular dynamics was calculated in the potential of the semiempirical MNDO method.

(6) The endohedral complex $\text{Li}@C_{60}^+$, whose electronic structure and equilibrium geometry were calculated in the restricted Hartree–Fock approximation by the semiempirical MNDO method (see [37]). The molecular dynamics was calculated in the potential of the semiempirical MNDO method.

(7) The endohedral complex $\text{H}_2@C_{36}$, whose electronic structure and equilibrium geometry were calculated in the restricted Hartree–Fock approximation by the nonsemiempirical Hartree–Fock method in the 3–21-G basis and by the semiempirical PM3 method. The structure of the polyhedron C_{36} in the complex was practically unchanged. The molecular dynamics was calculated in the potentials of the semiempirical PM3 method and in the nonempirical potential 3–21 G.

(8) The endohedral complex $\text{H}_2@C_{50}$, whose electronic structure and equilibrium geometry were calculated in the restricted Hartree–Fock approximation by the semiempirical PM3 method. The structure of the polyhedron C_{50} was chosen with the D_{5h} symmetry. The bond lengths were 0.1405 nm for the first type (6–6), 0.1378 nm for the second type (6–6), 0.1419 nm for the third type (6–5), 0.1474 nm for the fourth type (6–5), 0.1467 nm for the fifth type (6–5), and 0.1481 nm for the sixth type (5–5). The molecular dynamics was calculated in the potentials of the semiempirical PM3 method.

(9) The endohedral complex $\text{H}_2@C_{60}$, whose electronic structure and equilibrium geometry were calculated in the restricted Hartree–Fock approximation by

the semiempirical PM3 method. The molecular dynamics was calculated in the potentials of the semiempirical PM3 method.

(10) A number of endohedral complexes $\text{He}_n@C_{60}$, $n = 2, 3, 4$, whose electronic structure and equilibrium geometry were calculated in the restricted Hartree–Fock approximation by the semiempirical INDO method. The length of the 6–6 bond was 0.1397 nm, while the length of the 6–5 bond was 0.1449 nm. The molecular dynamics was calculated in the potential of the semiempirical INDO method.

All calculations of the complexes with light elements were made without taking into account the symmetry of the system. The optimization of the geometry of these complexes in all the methods was carried out with a convergence parameter of 0.01 kcal/mol per atom of the complex.

At the present time, the method of molecular dynamics [38], which does not require the introduction of empirical intermolecular and interatomic potentials for computations, is widely used for studying the dynamic properties of molecular systems. Car and Parinello [38] specially introduced the term “nonempirical molecular dynamics” to emphasize that the potential of the system is not chosen parametrically, but calculated by quantum-chemical (including semiempirical) methods for any configuration in the course of computer simulation. They used the demonstration version of the Hyper-Chem-5.02 program for calculations using the nonempirical molecular dynamics method, which makes it possible to make calculations based on *ab initio*, as well as a number of semiempirical (INDO, MNDO, PM3, etc.), potentials. The elegance of some programs (including Hyper-Chem) for implementing the molecular dynamics method is also worth noting. The software was developed so that successive variation of atomic coordinates with time can be observed in the form of a dynamic picture, which provides a visual and convenient representation of the results of computations.

In the approach of molecular dynamics, the electron system is described by a set of wave functions $\{\psi_i(\mathbf{r})\}$ belonging to the ground state of the Born–Oppenheimer potential surface at any instant, which allows us to describe the collective motion of electrons and nuclei corresponding to a set of coordinates $\{\mathbf{R}_j\}$. In this case, the fixed kinetic energy of electrons remains small as compared to the kinetic energy of ions, which makes it possible to calculate the forces acting on the nuclei at any instant with the help of the Hellman–Feynman theorem for the electron systems corresponding to instantaneous nuclear configurations. The equations of motion of the complete dynamic system including the fictitious electron dynamics and real

ion dynamics are determined by the Lagrangian

$$L = \mu \sum_i \int dr |\dot{\Psi}_i(r)|^2 + \frac{1}{2} \sum_l M_l \dot{R}_l^2 - E[\{\Psi_i\}, \{R_l\}, \{\alpha_v\}] + \sum_{i,j} \Lambda_{ij} (\int dr \Psi_i^*(r) \Psi_j(r) - \delta_{ij}) + \frac{1}{2} \sum_v \mu_v \dot{\alpha}_v^2,$$

where $E[\{\Psi_i\}, \{R_l\}, \{\alpha_v\}]$ is the total energy functional, which can be obtained using any quantum-chemical approach; the set $\{\alpha_v\}$ describes any possible external conditions, such as temperature, pressure, or volume; μ is the fictitious mass for the electron dynamics; and μ_v is an arbitrary parameter of the appropriate dimensions. The matrix $\Lambda_{i,j}$ is a set of Lagrangian multipliers ensuring the orthonormality of $\{\Psi_i(\mathbf{r})\}$. From these equations, we can obtain the Euler–Lagrange equations of motion

$$\begin{aligned} \mu \ddot{\Psi}_i(r, t) &= -\frac{\delta E}{\delta \Psi_i^*(r, t)} + \sum_k \Lambda_{ik} \Psi_k(r, t), \\ M_l \ddot{R}_l &= -\nabla_{R_l} E, \\ \mu_v \ddot{\alpha}_v &= -(\delta E / \delta \alpha_v), \end{aligned}$$

which describe the fictitious electron dynamics, ion dynamics, and the influence of external conditions (e.g., temperature), respectively.

The nonempirical molecular dynamics satisfies the Born–Oppenheimer approximation only under certain conditions. The situation with the choice of μ and other initial conditions for semiconductors and insulators is quite simple. However, a different situation prevails for systems in which the band gap is small and electrons interact strongly. This leads to thermal equilibrium between ions and electrons and violates the conditions of applicability of the Born–Oppenheimer approximation. In order to overcome these difficulties, the algorithm of thermostats [39] (one for ions and the other for electrons) is used in the nonempirical molecular dynamics. In this case, we have

$$\mu \ddot{\Psi}_i(t) = -\hat{H} f_i |\Psi_i(t)\rangle + \sum_k \Lambda_{ik} \Psi_k(t) - \mu \dot{\eta} |\Psi_i(t)\rangle,$$

where f_i is the occupancy, and

$$M_l \ddot{R}_l = -\nabla_{R_l} E - M_l \dot{\xi} \dot{R}_l.$$

The thermostat variables η and ξ are determined by the equations

$$\begin{aligned} Q_e \dot{\eta} &= \left[\mu \sum_i \langle \dot{\Psi}_i | \dot{\Psi}_i \rangle - E_e \right], \\ Q_R \dot{\xi} &= \left[\mu \sum_l M_l \dot{R}_l^2 - gkT \right], \end{aligned}$$

where Q_e and Q_R are the masses of the thermostats for the electron and ion components, respectively; E_e and T are the kinetic energy of electrons and the ionic temperature required by the conditions of the problem; and g is the number of degrees of freedom.

Time-dependent temperature fluctuations are included in the equations for the electron and ion thermostats, while the dynamics of the entire system obeys the principle of the thermodynamic-potential minimum. The simplest case of Newtonian dynamics describes the motion of the system in equilibrium, which allows us not only to study the dynamic properties of molecular and solid-state systems, but also to find effectively the equilibrium atomic structure.

It should be noted that, in the method of nonempirical molecular dynamics, the law of the conservation of energy (thermodynamic potential) is satisfied in the entire system, including in the electron and ion thermostats. This law can be written as

$$\begin{aligned} E &= \mu \sum_i \langle \dot{\Psi}_i | \dot{\Psi}_i \rangle + \frac{1}{2} \sum_l M_l \dot{R}_l^2 + E[\{\Psi_i\}, \{R_l\}] \\ &+ \frac{1}{2} Q_e \dot{\eta}^2 + \frac{1}{2} Q_R \dot{\xi}^2 + 2E_e \eta + gkT \xi, \end{aligned}$$

while the energy of the electron–nucleus system without thermostats is not conserved because of thermal fluctuations. Consequently, for systems with nonrigid atomic cores, situations are possible when thermal conditions affect the electronic structure and the spectra of the systems under investigation as a result of the violation of the energy conservation law, since different atomic configurations must have different electronic spectra. In particular, rapid temperature rearrangements in the electronic spectra must lead to superpositions of the spectra corresponding to different configurations, which must be manifested in broadening and blurring of a number of spectral features.

2. RESULTS OF CALCULATIONS AND DISCUSSION

The electronic structure of the C_{60} molecule, as well as its dynamic properties in various conditions and states, has been studied comprehensively (see table). According to the results of our molecular-dynamic calculations, the C_{60} molecule rotates about its center of mass as a single entity. The period of rotation τ and the frequency $\nu = 1/\tau$ were determined from the time variation of the coordinates of the atoms forming the carbon polyhedron. An analysis of a free C_{60} molecule proved that the frequency of its rotation at 300 K amounts to $0.79 \times 10^{10} \text{ s}^{-1}$. The experimental frequencies determined from the NMR spectra for the C_{60} molecule are $3.3 \times 10^{11} \text{ s}^{-1}$ in the gaseous phase at 300 K [28–30], $1.1 \times 10^{11} \text{ s}^{-1}$ in the solid phase at 300 K, and $5.0 \times 10^8 \text{ s}^{-1}$ below 260 K in the solid phase. It can be seen that our theoretical calculations based on the nonempir-

ical molecular dynamics method qualitatively describe the effect of the rotation of C_{60} molecules. The difference in the rotational frequencies is obviously due to the fact that semiempirical methods of calculations give, as a rule, exaggerated values of the energy and coupling constant and hence underestimate the change in the spacing between nuclei upon heating.

The rotation and the emergence of a nonzero orbital angular momentum of the entire molecule upon heating can be explained by the change in the total orbital angular momentum of the electron. Indeed, the total angular momentum of the system (the electron plus nuclear angular momenta) must be conserved, but an increase in temperature alters the effective nuclear spacing, and hence in the general form we can write

$$\langle \psi(r, R_0) | r \nabla | \psi(r, R_0) \rangle \neq \langle \psi(r, R_T) | r \nabla | \psi(r, R_T) \rangle.$$

This inequality holds since $\psi(r, R_0) \neq \psi(r, R_T)$, because the set of nuclear coordinates ($\{R_0\} \neq \{R_T\}$), which appear in the total electron wave function as parameters, changes with temperature. Consequently, the entire system must compensate for the change in the electron orbital angular momentum by the change in the ion orbital angular momentum, which is manifested in the rotation of molecules as a whole.

Nonempirical calculations of the lowest fullerene C_{36} in the 3- to 21-G basis at 300 K proved that this effect is also reproduced when the potential obtained by the *ab initio* method is used in the molecular dynamics. Since such computations require considerable time on computers, we could not estimate the rotational frequency of the molecule. As a matter of fact, the system is sort of "heated" in time due to the peculiarities of the algorithm in the molecular dynamics method using the system of thermostats. The typical time of heating is of the order of 0.2–0.3 ps, while a correct estimation of the rotational period can be made over time intervals equal to 0.5 ps. At the present time, the prevailing standard computer facilities do not allow us to carry out such a long simulation of the system behavior. The duration of intervals in our case was 0.1 ps, which required about two weeks of continuous operation of a P-II 450 Dual 256 MB RAM computer. The calculation of the rotational frequency of C_{36} using the semiempirical potential obtained using the PM3 method proved that the rotational frequency is slightly higher than for C_{60} and is equal to $3.2 \times 10^{10} \text{ s}^{-1}$.

The *ab initio* calculations of the equilibrium atomic structure of the hypothetical endohedral complex $H_2@C_{36}$ in the 3- to 21-G basis revealed that the hydrogen molecule is located at the center of the carbon polyhedron. Calculations based on the molecular dynamics method at 300 K also demonstrated the flexibility of the coordination of the H_2 molecule in the polyhedron. The hydrogen molecule moves in a multivalley potential, hopping from one minimum to another. Effectively, such motion appears as the rotation of a molecule in the C_{36} polyhedron. However, the rotational frequency also

Rotational frequencies of the Li_2 dimer and fullerene C_{60} in endohedral complexes $Li_2@C_{60}$ and $(Li_2@C_{60})_2$

Compound, temperature, K	Rotational frequency of Li_2 dimer, s^{-1}	Rotational frequency of fullerene C_{60} , s^{-1}
$Li_2@C_{60}$, 79	1×10^{12}	2.5×10^9
$Li_2@C_{60}$, 300	2.5×10^{12}	3.4×10^9
C_{60} , 300	–	7.9×10^9
Experimental frequency of rotation of the gas-phase C_{60} molecule at 300 K [28–30]	–	3.3×10^{11}
Experimental frequency of rotation of the C_{60} molecule in fullerite at 300 K [28–30]	–	1.1×10^{11}
Experimental frequency of rotation of the C_{60} molecule in fullerite below 260 K [28–30]	–	5.0×10^8

could not be estimated in this case in view of limitations of the computer facilities. An analysis of molecular dynamics in the semiempirical PM3 potential revealed that the hydrogen molecule rotates in the polyhedron at a frequency of $4 \times 10^{13} \text{ s}^{-1}$. It should be noted that the hydrogen molecule remains at the center of the carbon polyhedron.

An analysis of the dynamics of the hypothetical $H_2@C_{50}$ system shows that the rotational frequency of the hydrogen molecule in this endohedral complex is slightly lowered (to $3 \times 10^{13} \text{ s}^{-1}$) in view of the presence of a plateau on the potential surface within the carbon polyhedron. The hydrogen molecule is displaced by 0.09 nm from the center along the long axis of C_{50} in the course of its motion.

An analysis of the dynamics of the endohedral complex $H_2@C_{60}$ at 300 K proved that the hydrogen molecule in it does not rotate, but moves chaotically in the fullerene due to thermal fluctuations, which can be attributed to the presence of a large plateau (much larger than the hydrogen molecule) on the potential surface in the carbon polyhedron in all directions. For example, the displacement of the guest molecule from the center of C_{60} reaches 0.1 nm. An analysis of the system dynamics at 4 K revealed that the amplitude of motion of the hydrogen molecule decreases to 0.01 nm, but the system remains flexible all the same.

An analysis of the molecular dynamics for other interesting endohedral complexes of fullerene with helium atoms ($He_n@C_{60}$, $n = 2, 3, 4$) in the semiempirical INDO potential shows that such systems remain flexible at $T = 4 \text{ K}$, the rotational frequencies of helium atoms for these objects being estimated as $(3–5) \times 10^{12} \text{ s}^{-1}$. An increase in temperature to 300 K leads to a noticeable increase (up to $(6–7) \times 10^{12} \text{ s}^{-1}$) in the rotational frequency of the helium atoms. It should be noted

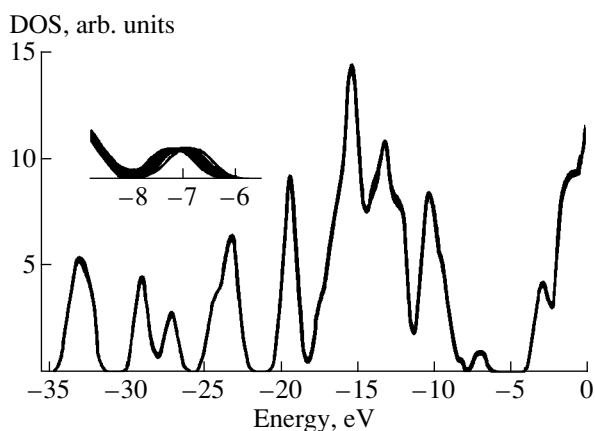


Fig. 2. Electronic structure observed in 16 stills of a dynamic picture superimposed and shot with a step of 0.01 ps calculated for the $\text{Li}_2@C_{60}$ complex at 300 K. It can be seen that the upper filled orbital (impurity electron state) changes its position with an amplitude of 1 eV. The inset shows the impurity state on a magnified scale.

that the carbon polyhedron in fact contains He_n molecules, the nuclear separation being 0.18 nm in all cases. (It should be noted that the calculation of the Van der Waals dimer He_2 by the INDO method gives 0.50 nm for the nuclear spacing, while in the *ab initio* approach (on the 6- to 31-G basis) this distance is 0.32 nm.)

Calculations of the electronic and atomic structures of Li-containing complexes show that lithium ions in the endohedral complex $\text{Li}_2@C_{60}$ are coordinated to the opposite vertices of the hexagons facing each other, so that the axis of the Li_2 fragment is just at the center of the polyhedron, the Li–Li separation being 0.299 nm, which is in accord with the C–C separation between the opposite carbon atoms from the base hexagons, while the Li–C distance (to carbon atoms belonging to hexagons) is 0.328 nm.

In the exohedral complex Li_2C_{60} , Li can be coordinated either to the center of a hexagon or to the center of a pentagon, the distance from the lithium ion being 0.232 nm to a carbon atom of the hexagon and 0.234 nm to a carbon atom of the pentagon.

In the endo-exohedral complex $\text{Li}[\text{Li}@C_{60}]$, the exohedral ion was coordinated to the center of a hexagon with the Li–C spacing equal to 0.231 nm, while the endohedral ion was coordinated to the center of a hexagon adjoining the hexagon to which the exohedral lithium is coordinated, the separation between the endohedral lithium ion and the carbon atom being 0.241 nm.

The coordination of lithium in the $\text{Li}@C_{60}^+$ complex takes place at the center of a hexagon, the Li–C distance being 0.2405 nm, while the separation between the lithium ion and the center of the hexagon is 0.1909 nm.

An analysis based on the molecular-dynamics method and the semiempirical potential demonstrates that endohedral Li ions in the $\text{Li}_2@C_{60}$ complex at 4 K

are “frozen” to a carbon wall. At a temperature above 79 K, a dynamic transition takes place, in which the ions are dislodged from the equilibrium geometry and start rotating in the polyhedron at a frequency of $1.0 \times 10^{12} \text{ s}^{-1}$, the carbon polyhedron itself also rotating at a frequency of $2.5 \times 10^9 \text{ s}^{-1}$. (It should be emphasized that this dynamic transition temperature is just an estimate of the potential barrier height rather than a thermodynamic parameter. It was mentioned above that all calculations were made by the molecular-dynamics method, which does not comprehensively take into account thermal fluctuations and in fact simulates the thermodynamic equilibrium state.) At 300 K, the rotational frequency increases and attains $2.5 \times 10^{12} \text{ s}^{-1}$ for lithium ions and $3.4 \times 10^9 \text{ s}^{-1}$ for the carbon polyhedron (see table).

According to the results of similar molecular-dynamic calculations, the exohedral complex Li_2C_{60} is rigid up to 300 K. The outer Li ions just vibrate near their equilibrium positions above the centers of both the hexagons and the pentagons.

The behavior of the endohedral ion in the endo-exohedral complex $\text{Li}[\text{Li}@C_{60}]$ is much more complicated: at 77 K, it changes its coordination from the center of a hexagon to the edge between two adjacent hexagons to which the exo- and endohedral ions were coordinated at 4 K. At 300 K, the endohedral ion starts migrating in a solid angle of the order of 30° in the region of coordination of the exohedral lithium.

The calculations made by the molecular dynamics method in a semiempirical potential show that the endohedral Li ion in the $\text{Li}@C_{60}$ complex at 300 K moves at a frequency of the order of $5 \times 10^{12} \text{ s}^{-1}$.

Let us now analyze the dependence of the electronic structure on the dynamic properties of the endohedral complex $\text{Li}_2@C_{60}$. Figure 2 presents the total densities of states plotted for 16 stills with an interval of 0.01 ps, obtained during dynamic filming of this complex. It can be seen that the impurity electronic state formed due to additional electrons supplied by Li atoms is “bloated.” The change in the energies of the upper filled orbital due to the change in the coordination of Li ions under the action of thermal fluctuations is quite large (of the order of 1 eV). The motion of Li ions also gives rise to a polarization wave at the carbon polyhedron. The motion of lithium ions causes a change in the sign of the carbon atoms, whose effective charges can vary from a few hundredths of the electron charge to fifteen hundredths of the electron charge.

Thus, the calculations made by the method of non-empirical molecular dynamics lead to the following conclusions.

(1) Endohedral complexes of fullerenes with closed shells and light guest atoms and molecules that are not connected through covalent bonds with the carbon walls are flexible systems.

(2) This property can be explained by the low (of the order of tens of kelvins) potential barriers on the potential surface of atomic rearrangements in carbon polyhedra.

(3) The motion of ions within polyhedra under the action of thermal fluctuations blurs the top of the valence band consisting of an impurity electronic state and generates a polarization wave on the surface of a carbon polyhedron, which moves behind positively charged guest ions.

The files with dynamic pictures have been placed on the server of the Institute of Physics, Siberian Division, Russian Academy of Sciences (Kirensky.krascience.rssi.ru). The authors can also send them by e-mail: paul@post.krascience.rssi.ru.

ACKNOWLEDGMENTS

This work was carried out at the Collective Center Quantum-Chemical Calculations of Nanoclusters at the Krasnoyarsk Research and Education Center for High Technologies, financed by the Federal Program Supporting Integration of Higher Education and Fundamental Research, grant no. 69. This study was supported by the Russian Foundation for Basic Research for support, project no. 97-03-33684a, the State Program on HTSC, project no. 99019, and the State program "Fullerenes and Atomic Clusters," project no. 97018, and also the NATO Scientific Affairs Division, project PST.CLG 974818.

REFERENCES

1. A. V. Eletskiĭ and B. M. Smirnov, *Usp. Fiz. Nauk* **165** (9), 977 (1995).
2. C. T. White, J. W. Mintmire, R. C. Mowrwy, *et al.*, in *Buckminsterfullerenes*, Ed. by W. E. Billups and M. A. Ciufolini (VCH, New York, 1993).
3. W. Andreoni, *Annu. Rev. Phys. Chem.* **49**, 405 (1998).
4. A. R. Ramírez, *Supercond. Rev.* **1** (1–2), 1 (1994).
5. N. Krawez, A. Gromov, R. Tellgmann, and E. E. B. Campbell, in *Proceedings of XII International Winter School on Electronic Properties of Novel Materials—Progress in Molecular Nanostructures, Kirchberg, Tirol, 1998* (American Institute of Physics, Woodbury, 1998), p. 368.
6. Y. Yoshinari, H. Alloul, V. Brouet, *et al.*, *Phys. Rev. B* **54** (9), 6155 (1996).
7. T. Pichler, M. S. Golden, M. Knupfer, and J. Fink, in *Proceedings of the XII International Winterschool Electronic Properties of Novel Materials, 1998*, Ed. by H. Kuzmany, p. 271.
8. D. M. Poirier, M. Knupfer, J. H. Weaver, *et al.*, *Phys. Rev. B* **49** (24), 17403 (1994).
9. J. H. Weaver, *Acc. Chem. Res.* **25** (3), 143 (1992).
10. M. Takata, B. Umeda, E. Nishibori, *et al.*, *Nature* **377**, 46 (1995).
11. W. Sato, K. Sueki, K. Kikuchi, *et al.*, *Phys. Rev. B* **58** (16), 10850 (1998).
12. C. Gu, F. Stepniak, D. M. Poirier, *et al.*, *Phys. Rev. B* **53** (3), 1196 (1995).
13. J. Chioslovski and E. D. Fleischmann, *J. Chem. Phys.* **94** (5), 3730 (1991).
14. A. B. Roitsin, L. V. Artamonov, and A. A. Klimov, *Fiz. Nizk. Temp.* **23** (10), 1112 (1997) [*Low Temp. Phys.* **23**, 835 (1997)].
15. H. Mauser, T. Clark, and A. Hirsch, in *Proceedings of the XII International Winterschool on Electronic Properties of Novel Materials, 1998*, Ed. by H. Kuzmany, p. 202.
16. C. G. Joslin, J. Yang, C. G. Gray, and J. D. Poll, *Chem. Phys. Lett.* **211** (6), 587 (1993).
17. L. Pang and F. Brisse, *J. Phys. Chem.* **97** (33), 8562 (1993).
18. Y. S. Li and D. Tomanek, *Chem. Phys. Lett.* **221** (5), 453 (1994).
19. D. Tomanek and Y. S. Li, *Chem. Phys. Lett.* **243** (1), 42 (1995).
20. V. A. Levashov, A. A. Remova, and V. R. Belosludov, *Pis'ma Zh. Éksp. Teor. Fiz.* **65** (8), 647 (1997) [*JETP Lett.* **65**, 683 (1997)].
21. Y. Maruyama, K. Ohno, K. Esfarjani, and Y. Kawazoe, *Sci. Rep. Res. Inst. Tohoku Univ., Ser. A* **41** (2), 183 (1996).
22. A. H. H. Chang, W. C. Ermler, and R. M. Pitzer, *J. Chem. Phys.* **94** (7), 5004 (1991).
23. J. Liu and S. Iwata, *Phys. Rev. B* **50** (8), 5552 (1994).
24. F. De Proft, C. van Alsenoy, and P. Geerlings, *J. Phys. Chem.* **100** (18), 7440 (1996).
25. S. Parchkovskii and W. Thiel, *J. Chem. Phys.* **106** (5), 1796 (1997).
26. Y. Wang and D. Tomanek, *Chem. Phys. Lett.* **208** (1–2), 79 (1993).
27. B. I. Dunlop, J. L. Ballester, and P. P. Schmidt, *J. Phys. Chem.* **96** (24), 9781 (1992).
28. Y. Maniwa, K. Mizoguchi, K. Kume, *et al.*, *Solid State Commun.* **80** (12), 609 (1991).
29. R. D. Johnson, C. S. Yannoni, H. C. Dorn, *et al.*, *Science* **225**, 1235 (1992).
30. R. Tycko, G. Dabbagh, R. M. Fleming, *et al.*, *Phys. Rev. Lett.* **67** (14), 1886 (1991).
31. P. A. Heiney, J. E. Fischer, A. R. McGhi, *et al.*, *Phys. Rev. Lett.* **66** (22), 2911 (1991).
32. R. Moret, P. A. Albouy, V. Agafonov, *et al.*, *J. Phys. I* **2** (5), 511 (1992).
33. W. Andreoni and A. Curioni, *Phys. Rev. Lett.* **77** (5), 834 (1996).
34. W. Andreoni and A. Curioni, *Appl. Phys. A* **A66**, 299 (1998).
35. J. L. Ballester and B. I. Dunlop, *Phys. Rev. A* **45** (10), 7985 (1992).
36. M. W. Schmidt, K. K. Baldrige, and J. A. Boatz, *J. Comput. Chem.* **14** (6), 1347 (1993).
37. S. A. Varganov, P. V. Avramov, and S. G. Ovchinnikov, *Fiz. Tverd. Tela (St. Petersburg)* **42** (2), 378 (2000) [*Phys. Solid State* **42**, 388 (2000)].
38. R. Car and M. Parinello, *Phys. Rev. Lett.* **55** (22), 2471 (1985).
39. P. E. Blochl and M. Parinello, *Phys. Rev. B* **45** (11), 9413 (1992).

Translated by N. Wadhwa